

# Search for a Standard Model-like Higgs boson decaying to WW or ZZ in the mass range 145 to 1000 GeV

---

**Dermot MORAN\***

†

*Departamento de Física Teórica, Universidad Autónoma de Madrid (ES)*

*E-mail:* [dermot.anthony.moran@cern.ch](mailto:dermot.anthony.moran@cern.ch)

A search for a heavy Higgs boson using several final states in the  $H \rightarrow WW$  and  $H \rightarrow ZZ$  decay channels is reported. The search is based upon proton-proton collision data samples corresponding to an integrated luminosity of up to  $5.1 \text{ fb}^{-1}$  at  $\sqrt{s} = 7 \text{ TeV}$  and up to  $19.7 \text{ fb}^{-1}$  at  $\sqrt{s} = 8 \text{ TeV}$ , recorded by the CMS experiment at the CERN LHC. A Higgs boson with Standard Model-like couplings and decays in the mass range of  $145 \text{ GeV} < m_H < 1000 \text{ GeV}$  is excluded at 95% confidence level. The results are also interpreted in the context of an electroweak singlet extension of the Standard Model.

*XXIII International Workshop on Deep-Inelastic Scattering  
27 April - May 1 2015  
Dallas, Texas*

---

\*Speaker.

†Representing the CMS Collaboration.

## 1. Introduction

The Standard Model (SM) of electroweak (EW) interactions posits the existence of the Higgs boson, a scalar particle associated with the field responsible for spontaneous EW symmetry breaking [1] [2]. In 2012 the ATLAS and CMS collaborations at the CERN LHC reported the observation of a new boson with a mass of about 125 GeV [4] [5]. Subsequent studies of the production and decay rates and of the spin-parity quantum numbers of the new boson, denoted as  $h(125)$ , show that its properties are compatible with those expected for the SM Higgs boson. Nevertheless, there is a possibility that the newly discovered particle is part of a larger Higgs boson sector and thus only partially responsible for EW symmetry breaking. This can be realized in several scenarios, such as two Higgs-doublet models [6], or models in which the SM Higgs boson mixes with a heavy EW singlet scalar [7], which predict the existence of additional resonances at high mass, with couplings similar to those of the SM Higgs boson.

A search for a heavy SM-like Higgs boson has been conducted by the CMS experiment [3] in the mass range  $145 \text{ GeV} < m_H < 1000 \text{ GeV}$ . The analysis is based upon proton-proton collision data, corresponding to integrated luminosities of up to  $5.1 \text{ fb}^{-1}$  at  $\sqrt{s} = 7 \text{ TeV}$  and up to  $19.7 \text{ fb}^{-1}$  at  $\sqrt{s} = 8 \text{ TeV}$ . The dominant production mechanisms, gluon fusion ( $ggF$ ,  $gg \rightarrow H$ ) and vector boson fusion (VBF,  $qq \rightarrow qqH$ ), and the dominant decay channels,  $H \rightarrow WW$  and  $H \rightarrow ZZ$ , for a heavy SM-like Higgs are explored.

In addition to a heavy SM-like Higgs boson search, the data are also interpreted in the context of an expanded Higgs sector with an additional EW singlet.

## 2. Analysis Overview

In the case of a Higgs boson decaying into a pair of Z bosons, final states containing four charged leptons ( $ZZ \rightarrow \ell^- \ell^+ \ell'^- \ell'^+$ ) [4] [12], two charged leptons and a quark-antiquark pair ( $ZZ \rightarrow \ell^- \ell^+ q\bar{q}$ ), and two charged leptons and two neutrinos ( $ZZ \rightarrow \ell^- \ell^+ \nu\bar{\nu}$ ) [13] are considered, where  $\ell = e$  or  $\mu$  and  $\ell' = e, \mu$  or  $\tau$ . For a Higgs boson decaying into two W bosons, the fully leptonic ( $WW \rightarrow \ell^- \bar{\nu} \ell^+ \nu$ ) [14] and semileptonic ( $WW \rightarrow \ell \nu q\bar{q}$ ) final states are considered. Several Monte Carlo generators are used to simulate the signals and their background processes. The effect of interference between signal and SM background processes is taken into account by correcting the simulated diboson invariant mass lineshape to match theoretical predictions [8] [9].

The analyses utilise jet multiplicity categories including VBF categories which require the presence of a pair of jets with a topology consistent with VBF production. The categories are characterized by different signal yields and signal-to-background ratios and increase the sensitivity of the overall analysis.

At high Higgs boson masses, the  $p_T$  of the Z or W boson is high enough that the quark-antiquark pair from a hadronic decay are reconstructed as a single merged jet. To identify merged jets with 2 sub-jets and to improve the jet mass resolution a number of novel jet substructure techniques are implemented [10].

For a number of channels it is possible to exploit the angular distributions of the final state particles. These distributions are sensitive to the spin-parity of the Higgs and so are exploited to discriminate between signal and background [11].

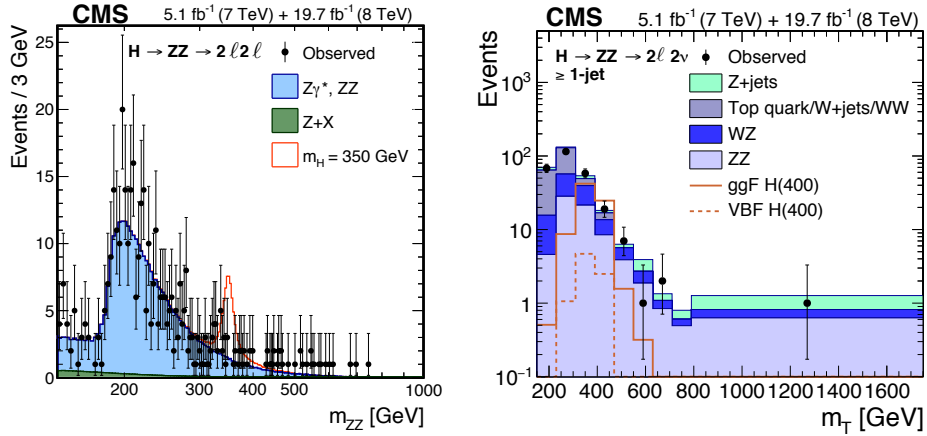


**Figure 1:** The left hand plot shows the diboson invariant mass distribution for the  $H \rightarrow ZZ \rightarrow \ell^- \ell^+ \ell^- \ell^+$  final state. The right hand plot shows the  $m_T$  distribution for the  $H \rightarrow ZZ \rightarrow \ell^- \ell^+ \nu \bar{\nu}$  channel in events with at least one jet. Points represent the observed data, the shaded histograms represent the background and the unshaded histogram the signal expectations.

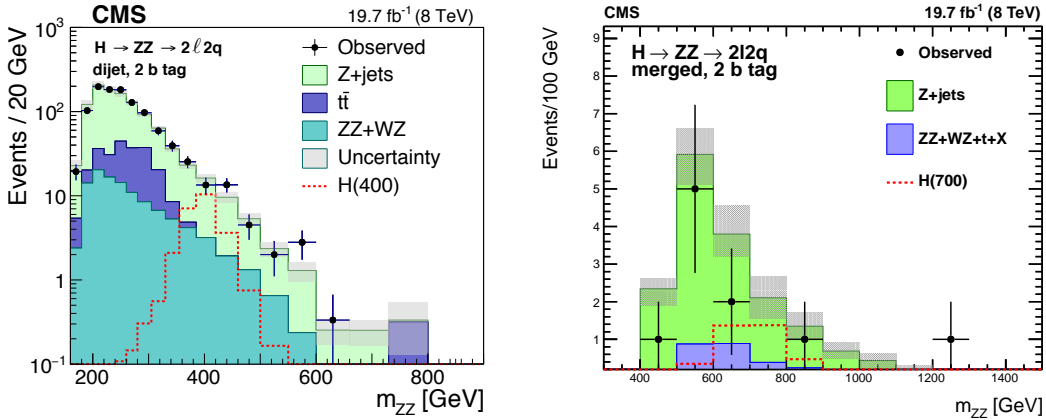


**Figure 2:** Distributions of the diboson invariant mass for the  $H \rightarrow ZZ \rightarrow \ell^- \ell^+ q\bar{q}$  final state in the dijet 2-btag category (left) and in the merged jet 2-btag category (right). Points represent the observed data, the shaded histograms represent the background and the unshaded histogram the signal expectations.

## 2.1 $H \rightarrow ZZ$ Channels

The  $H \rightarrow ZZ \rightarrow \ell^- \ell^+ \ell^- \ell^+$  final state is fully reconstructed with a experimental mass resolution of 1-2%, it has extremely low background and a high selection efficiency. A kinematic discriminant is implemented which exploits the angular distributions of the final state particles and the masses of the reconstructed Z bosons. The final signal search is performed fitting the invariant mass of the 4 lepton system and the kinematic discriminant. The left hand plot in Figure 1 displays the diboson invariant mass for selected events in this channel.

The  $H \rightarrow ZZ \rightarrow \ell^- \ell^+ \nu \bar{\nu}$  channel has a relatively large branching fraction. As one of the Z

bosons decays to neutrinos the final state contains large missing transverse energy  $E_T^{miss}$  [16]. The mass peak is not reconstructable in this channel, instead the transverse mass,  $m_T$ , of the dilepton and  $E_T^{miss}$  system is adopted. The final results are extracted fitting the  $m_T$  and  $E_T^{miss}$  distributions with selections adjusted for different  $m_H$  hypotheses. The right hand plot in Figure 1 shows the  $m_T$  distribution in events with at least one jet.

The  $H \rightarrow ZZ \rightarrow \ell^- \ell^+ q\bar{q}$  final state has the largest  $H \rightarrow ZZ$  branching fraction and the final state is also fully reconstructed (with a typical experimental mass resolution of about 3%), however it has a large background contribution from  $Z$ +jets production. To ensure sensitivity over the Higgs mass range of interest both dijets and merged jets are used to reconstruct the hadronic  $Z$  decay. In order to exploit the different jet composition of signal and background, events are classified according to the number of  $b$  tagged jets [15] (or sub-jets in the case of merged jet reconstruction). Also a likelihood discriminant based on the angular distribution of the final state particles is used to separate signal-like from background-like events. The diboson invariant mass is fitted to perform the final signal search. Figure 2 shows the mass distribution for events in the dijet 2-btag category (left) and for events in the merged jet 2-btag category (right).

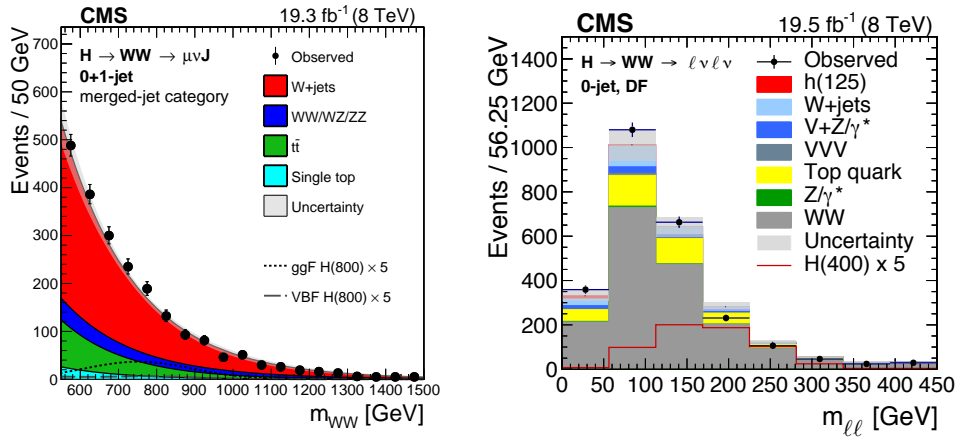


**Figure 3:** The left hand plot shows the diboson invariant mass distribution for the 0+1-jet category of the  $H \rightarrow WW \rightarrow \ell\nu q\bar{q}$  channel. The right hand plot shows the dilepton mass distribution for the 0-jet DF category of the  $H \rightarrow WW \rightarrow \ell^- \bar{\nu} \ell^+ \nu$  channel. Points represent the observed data, shaded graphs represent the background and open histograms represent the signal expectations.

## 2.2 $H \rightarrow WW$ Channels

The largest branching fraction of all channels considered belongs to the  $H \rightarrow WW \rightarrow \ell\nu q\bar{q}$  channel, however it has a large background from  $W$ +jets production. The hadronic  $W$  decay is reconstructed using both dijets and merged jets, insuring sensitivity over the Higgs mass range of interest. A likelihood discriminant is implemented exploiting the angles between the Higgs boson decay products and the lepton charge. The diboson invariant mass, which is used for the final signal search, is computed using a neutrino longitudinal momentum that is determined from the constraint that the leptonically decaying  $W$  boson is produced on-shell. The left hand plot in Figure 3 displays the invariant mass for events with less than 2 additional jets.

The  $H \rightarrow WW \rightarrow \ell^- \bar{\nu} \ell^+ \nu$  channel contains large  $E_T^{miss}$  due to the undetected neutrinos. As well as in jet multiplicity categories, signal candidates are divided into same-flavor (SF) dilepton and different-flavor (DF) dilepton categories. The final analysis is performed by fitting the dilepton invariant mass and the transverse mass. The right hand plot in Figure 3 shows the dilepton invariant mass for events in the 0-jet DF category,

### 3. Results

No significant excess over the expected SM background has been observed in any of the final states. The combination of all the measurements requires the simultaneous analysis of the data selected by all individual analysis channels, accounting for all statistical and systematic uncertainties, as well as their correlations. The main sources of systematic uncertainties arise from the assumptions in the signal model, the objects reconstruction used in the analysis, and several common experimental sources. Upper limits on the model parameters are computed for different  $m_H$  hypotheses using the  $CL_s$  modified frequentist method [17].

#### 3.1 SM-like Higgs Boson Search

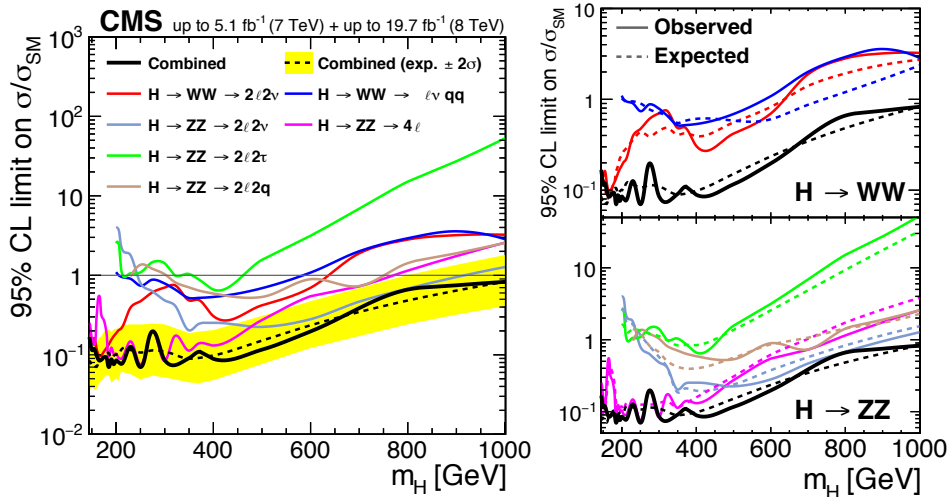


**Figure 4:** The upper limits at 95% CL on the production cross section relative to the SM for a heavy Higgs boson with SM-like couplings for each of the contributing final states and their combination. Observed and expected limits for the individual channels are shown in the right, for WW channels on top and ZZ channels on the bottom.

The combined results obtained for a heavy Higgs boson with SM-like couplings for all the different contributing final states are displayed in Figure 4. The observed 95% CL limit is shown for each final state. In the plot on the left the expected combined 95% CL limit of the six channels is plotted as a dashed black line, while the yellow shaded region represents the  $\pm 2\sigma$  uncertainty in the expected limit. The plot on the right shows the channel by channel comparison of the expected and observed limit, using the same color legend. The top right plot refers to the WW final states, while the bottom right plot refers to the ZZ final states.

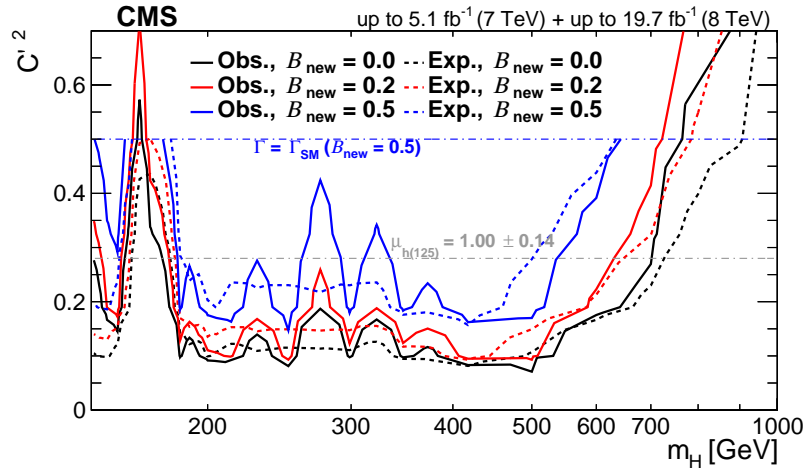


**Figure 5:** The 95% CL upperlimits on  $C'^2$  in the EW singlet scenario, as a function of the heavy Higgs boson mass, for several  $B_{new}$  values. The upper blue dashed line represents where, for  $B_{new} = 0.5$ , the variable width of the heavy Higgs boson reaches the width of a SM-like Higgs boson. The lower grey dash-dotted line shows the indirect lower limit on  $C'^2$  obtained from the  $h(125)$  signal strength measurement.

The combined limit on the cross section times the branching ratio excludes at 95% CL the presence of a SM-like Higgs boson across the full range of  $145 \text{ GeV} < m_H < 1000 \text{ GeV}$ .

### 3.2 EW Singlet Higgs Boson Search

In the EW singlet scenario, the couplings of the  $h(125)$  and the high mass Higgs boson are constrained by unitarity and the coupling of  $h(125)$  is therefore lower than in the SM case. Unitarity is enforced by the relation  $C'^2 + C^2 = 1$ , where  $C^2$  and  $C'^2$  are the scale factors of the couplings of  $h(125)$  and the high mass Higgs boson, respectively, with respect to the SM. The focus of this interpretation is limited to the case where  $C'^2 \leq (1 - B_{new})$ , where  $B_{new}$  is the contribution to the heavy Higgs boson width of non-SM decays. In this regime the new state is expected to have an equal or narrower width with respect to the SM case.

Figure 5 shows the observed and expected upper limit on  $C'^2$  as a function of the heavy Higgs mass, for several  $B_{new}$  values. In the same plot, the indirect limit on  $C'^2$  obtained using the signal strength fits to the  $h(125)$  boson is shown. The upper blue dashed line represents where, for  $B_{new} = 0.5$ , the variable width of the heavy Higgs boson reaches the width of a SM-like Higgs boson.

## 4. Conclusion

The results of a search for a heavy Higgs boson in  $H \rightarrow WW$  and  $H \rightarrow ZZ$  decay channels, for Higgs boson mass hypotheses in the range  $145 \text{ GeV} < m_H < 1000 \text{ GeV}$ , have been presented. No significant excess over the expected SM background has been observed in any of the final states. In the case of the search for a heavy Higgs boson with SM-like couplings and decays, the existence of such a heavy Higgs boson over the entire search range of  $145 \text{ GeV} < m_H < 1000 \text{ GeV}$  is excluded at 95% CL. This represents the completion of one of the priority measurements of Run 1, the search

for Higgs bosons up to 1 TeV. The observed data is also interpreted in the context of a EW singlet in addition to the 125 GeV Higgs boson. A sizeable region of the parameter space is excluded.

## References

- [1] F. Englert and R. Brout, Broken Symmetry and the Mass of Gauge Vector Mesons, *Phys. Rev. Lett.* 13 (1964) 321, doi:10.1103/PhysRevLett.13.321.
- [2] P. W. Higgs, Broken symmetries, massless particles and gauge fields, *Phys. Lett.* 12 (1964) 132, doi:10.1016/0031-9163(64)91136-9.
- [3] CMS Collaboration, The CMS experiment at the CERN LHC, *JINST* 3 (2008) S08004, doi:10.1088/1748-0221/3/08/S08004.
- [4] CMS Collaboration, Observation of a new boson at a mass of 125 GeV with the CMS experiment at the LHC, *Phys. Lett. B* 716 (2012) 30, doi:10.1016/j.physletb.2012.08.021, arXiv:1207.7235.
- [5] ATLAS Collaboration, Observation of a new particle in the search for the Standard Model Higgs boson with the ATLAS detector at the LHC, *Phys. Lett. B* 716 (2012) 1, doi:10.1016/j.physletb.2012.08.020, arXiv:1207.7214.
- [6] G. C. Branco et al., Theory and phenomenology of two-Higgs-doublet models, *Phys. Rept.* 516 (2012) 1, doi:10.1016/j.physrep.2012.02.002, arXiv:1106.0034.
- [7] V. Barger et al., CERN LHC phenomenology of an extended Standard Model with a real scalar singlet, *Phys. Rev. D* 77 (2008) 035005, doi:10.1103/PhysRevD.77.035005, arXiv:0706.4311.
- [8] S. Goria, G. Passarino, and D. Rosco, The Higgs-boson lineshape, *Nucl. Phys. B* 864 (2012) 530, doi:10.1016/j.nuclphysb.2012.07.006, arXiv:1112.5517.
- [9] N. Kauer and G. Passarino, Inadequacy of zero-width approximation for a light Higgs boson signal, *JHEP* 08 (2012) 116, doi:10.1007/JHEP08(2012)116, arXiv:1206.4803.
- [10] CMS Collaboration, Identification techniques for highly boosted W bosons that decay into hadrons, *JHEP* 12 (2014) 017, doi:10.1007/JHEP12(2014)017, arXiv:1410.4227.
- [11] Y. Gao et al., Spin determination of single-produced resonances at hadron colliders, *Phys. Rev. D* 81 (2010) 075022, doi:10.1103/PhysRevD.81.075022, arXiv:1001.3396.
- [12] CMS Collaboration, Search for the Standard Model Higgs boson in the  $H \rightarrow ZZ \rightarrow ll\tau\tau$  decay channel in pp collisions at  $\sqrt{s} = 7$  TeV, *JHEP* 03 (2012) 081, doi:10.1007/JHEP03(2012)081, arXiv:1202.3617.
- [13] CMS Collaboration, Search for the Standard Model Higgs boson in the  $H \rightarrow ZZ \rightarrow 2l2\nu$  channel in pp collisions at  $\sqrt{s} = 7$  TeV, *JHEP* 03 (2012) 040, doi:10.1007/JHEP03(2012)040, arXiv:1202.3478.
- [14] CMS Collaboration, Measurement of Higgs boson production and properties in the WW decay channel with leptonic final states, *JHEP* 01 (2014) 096, doi:10.1007/JHEP01(2014)096, arXiv:1312.1129.
- [15] CMS Collaboration, Identification of b-quark jets with the CMS experiment, *JINST* 8 (2013) P04013, doi:10.1088/1748-0221/8/04/P04013, arXiv:1211.4462.
- [16] CMS Collaboration, Missing transverse energy performance of the CMS detector, *JINST* 6 (2011) P09001, doi:10.1088/1748-0221/6/09/P09001, arXiv:1106.5048
- [17] A. L. Read, Modified frequentist analysis of search results (the  $CL_s$  method), CERN Report CERN-OPEN-2000-005, 2000.